IEEE Access
Multidisciplinary | Rapid Review | Open Access Journal

Received May 3, 2019, accepted May 27, 2019, date of publication June 11, 2019, date of current version July 1, 2019.

Digital Object Identifier 10.1109/ACCESS.2019.2920232

System Design and Optimization of In-Route Wireless Charging Infrastructure for Shared Automated Electric Vehicles

AHMED A. S. MOHAMED, (Senior Member, IEEE), ANDREW MEINTZ, AND LEI ZHU
National Renewable Energy Laboratory, Golden, CO 80401, USA

Corresponding author: Ahmed A. S. Mohamed (Ahmed.Mohamed@nrel.gov)

This work was supported by the U.S. Department of Energy Office of Energy Efficiency and Renewable Energy Vehicle Technologies Office (VTO) under the Systems and Modeling for Accelerated Research in Transportation (SMART) Mobility Laboratory Consortium, an initiative of the Energy Efficient Mobility Systems (EEMS) Program.

ABSTRACT Deploying shared automated electric vehicles (SAEVs) on current roadways in cities will significantly shape current transportation systems and make our urban mobility systems more efficient, convenient, and environmentally friendly. Utilizing wireless power transfer (WPT) technology to charge the SAEVs provides perfect fits for realizing a fully automated mobility system. However, the investment in wireless charging infrastructure (WCI) presents a critical barrier for commercializing and adopting this technology. The barrier can be cleared by realizing the proper design of the WPT system that maximizes the benefits and minimizes the cost of WCI at the same time. This paper introduces a system design optimization tool and methodology for WCI for serving fixed-route SAEVs in automated mobility districts (AMDs). The tool offers the capability of integrating driving data (simulated or collected from the real world), vehicle parameters (e.g., battery, motor, dimensions, and so on), and wireless charger characteristics (rate, locations, alignment, and so on) to generate energy and state-of-charge profiles for each vehicle, considering motoring, regenerative braking, and charging. Furthermore, the proposed tool incorporates a multi-objective optimization layer for searching the optimum design parameters based on predefined objectives and constraints. The proposed method was utilized to design the WCI for a hypothetical AMD scenario with four SAEVs. The outcomes show that implementing in-route wireless chargers at designated stops for the SAEVs with maximum power level has the potential to provide a charge sustaining operation with 52% reduction in the on-board battery and presents the most cost-effective solution. The proposed solution is assessed in comparison with other charging technologies, such as stationary WPT and dc fast charging, and it shows the most feasible option for an AMD network in terms of cost, convenience, and performance.

INDEX TERMS Automated mobility district, in-route, shared automated electric vehicles, wireless charging infrastructure, wireless power transfer.

I. INTRODUCTION

Recently, three revolutions in the transportation sector —automation, shared mobility, and electrification—have the potential to reduce energy/fuel consumption and greenhouse gas emissions. Shared automated electric vehicle (SAEV) technology is bringing a significant reduction in vehicle emissions, and energy use by decreasing vehicle miles traveled and accelerating the adoption of cleaner vehicles and fuels [1]. SAEVs will unprecedentedly change current transportation systems and make our urban mobility systems more efficient, convenient, and environmentally friendly [2]. However, the proliferation of SAEVs could be hindered if electric vehicle (EV) charging infrastructure is not able to support an influx of high-mileage, high-usage SAEVs. Based on the literature, there are three alternatives for EV supply equipment (EVSE), i.e., charging infrastructure [3]: 1) battery swapping stations, 2) conductive charging stations, and 3) wireless charging. In a battery swapping scenario, the battery swapping stations (BSSs) are set

The associate editor coordinating the review of this manuscript and approving it for publication was Shagufta Henna.

up to replace the empty battery of the vehicle with a fully charged one [4]. This strategy offers a speedy recharging process (i.e., battery exchange in less than five minutes), and it allows flexible charging time, which can be shifted to the off-peak period. However, the long-term battery health impacts, associated cost, and practicality of BSSs are still in question [3]. Although conductive charging technology offers a cost-effective and feasible solution [5], it requires a longer charging time, and it is inconvenient for autonomous vehicles since it requires someone to plug in the vehicle, which causes extra labor load in the case of driverless vehicles. These limitations can be avoided by implementing fast chargers with a robot-based plug-in in which an automated arm will plug in the vehicle, instead of needing a human [6], [7]. Even though this seems a logical solution; the conductive charging technology still requires dedicated land or space for charging stations, which is challenging in crowded cities and city districts. In addition, it does not solve the limited driving range of EVs unless a large battery is installed in the vehicle, which means a heavier, larger, and more expensive vehicle. Besides, heavy-duty cables exposed to the public may lead to safety issues, such as arcing and exposed conductor [8]. The third option is the wireless (inductive) power transfer (WPT) in which the vehicle can be charged by magnetic induction during either long-term parking (stationary), driving (dynamic or in-motion), or transient stops (quasi-dynamic or opportunistic). Wireless charging technology offers an ideal solution for SAEV charging to accommodate its automation. The wireless charging infrastructure (WCI) can be implemented on the road and does not require dedicated stations, and it is safe because no heavy-duty cables are needed [9], [10]. Furthermore, implementing dynamic wireless power transfer (DWPT) has the potential to provide infinite driving range and to dramatically reduce a vehicle's battery size, which will benefit the SAEV adoption. Therefore, wireless charging technology is considered in this work for serving SAEVs.

One of the main limitations of the wireless charging technology is the high initial investment cost compared to the conventional conductive charging. However, this large initial cost can be compensated by decreasing the battery size and increasing vehicle range due to the elimination of recharging downtime [11]. Therefore, optimizing the system key design parameters of this technology is critical to make it cost-efficient for SAEVs. Several works have been introduced in the literature about component design and optimization of stationary WPT technology, including power pads, power electronics converters, and compensation networks [12]–[17]. Others investigated component design in dynamic WPT technology, such as [18]–[23]. In [11], the system design of the online line electric vehicle (OLEV) developed by the Korea Advanced Institute of Science and Technology (KAIST) was investigated, considering a shuttle bus service in the Seoul Grand (Amusement) Park. In [24], another design optimization was presented for the OLEV system operating at the KAIST campus. The researchers developed a mathematical model for the OLEV project and utilized it to define the optimum battery capacity and wireless track allocation. This work indicated promising results for the specific case of an OLEV bus and would not be appropriate for scenarios that use SAEVs because of the consideration of regulated speed profile, fixed charging power, and neglecting several vehicle dynamics, such as regenerative braking. Another optimization approach for the vehicle parameters (cost and size) with a dynamic WPT charger was presented in [25]. In [26], the authors performed a system optimization algorithm for implementing dynamic WPT technology at highways, which was applied to constant speed scenarios and did not consider sizing the battery capacity. Researchers from the National Renewable Energy Laboratory (NREL) investigated WCI design for serving circulator shuttles operating at the NREL campus [27], and the shuttle system at Zion National Park, Utah, USA [28]. In those works, the researchers conducted parametric analyses for charging power and battery capacity, considering few positions for stationary WPT system.

In contrast to the works mentioned above, this paper proposes an advanced design optimization tool for determining the key parameters of the WPT system serving fixed-route on-demand SAEVs operating in automated mobility districts (AMDs). The contributions in this work are summarized as follows:

- Developing a microscopic simulation model for SAEVs operating in AMDs.
- Integrating the simulated driving data with a vehicle energy consumption model, considering a real autonomous electric shuttle EasyMile EZ10 parameters, and a wireless charger power model, considering the vehicle position in both travel and lane directions.
- Proposing an optimization layer to automatically find the best combination of the system key design parameters, including battery capacity, charging power, placement location, track length, etc.
- Formulating and solving a multi-objective optimization problem that guarantees a charge sustaining operation with minimum cost and proper battery capacity while avoiding overcharging and charge depletion.
- Evaluating the proposed in-route charging solution in comparison with other technologies, including stationary WPT and dc fast charger (DCFC).

II. MODELING OF AUTOMATED MOBILITY DISTRICTS

A. AUTOMATED MOBILITY DISTRICTS

Deploying SAEV technology will mutate our transportation systems and make urban mobility safer, more efficient, convenient, and environmentally friendly. However, to realize such a future transportation system powered by SAEVs anywhere in smart cities may not be trivial and may take time due to the maturity of SAEV technology and its deployment. On one hand, SAEVs or automated shuttles (ASs) have already been implemented in specific places (e.g., airports),

such as automated person movers (APMs), personal rapid transit (PRT), and group rapid transit (GRT). Those systems usually require expensive additional infrastructure, such as exclusive guideways for ASs, and some even need specially designed vehicles. They are not easy to replicate anywhere in current cities. Along this line, AMDs describing a district-scale (such as 5 to 10 miles squared) implementation of SAEV technology to realize the full benefits of automated-shared-mobility services within a confined geographic region was raised by researchers from NREL [2], [29]. An AMD could be considered as an intermediate step towards anywhere automated vehicle service in cities. Comparing with current PRT-like systems, AMDs use current existing roadway infrastructure and is suitable for various automation levels of ASs. In an AMD, autonomous electric shuttles serve most of the mobility demand in the district. Personal vehicle use is not encouraged because of parking availability and pricing or prohibited by disallowing mobility access by privately owned vehicles.

B. AMD SIMULATION

Because no real AMD networks exist, a hypothetical diamond network is considered and modeled in the Simulation of Urban Mobility (SUMO) microscopic traffic tool [30]. It has 13 nodes and 48 links, as shown in Fig. 1. The hypothetical network is chosen in this study as an example for future AMD scenarios, which includes all the expected automated electric mobility elements for an AMD, such as automated electric shuttles (AESs), fixed-route on-demand service, and AES stops but does not have the traffic network complexity. The network is generated by the *netgenerate* module from the SUMO package. The nodes represent the junctions of the road network, and the links (or edges) indicate the roadways between the junctions. Each edge is directional and consists of two motor vehicle lanes and one pedestrian lane. Four on-demand AESs are running on fixed routes in the middle loop (shown with yellow dashed line) on the network. Two AESs operate in the clockwise direction of the loop, while the other two serve the demand in the counter-clockwise direction. Each edge in the circuit has a pedestrian sidewalk lane and has an AES stop (located inside the white boxes and denoted as pink segments). Three traffic lights/signals are assigned at the intersections, depicted by the red boxes, and their traffic signal timing configurations are set by default as provided by SUMO. The default traffic signal timing is designed according to the related edge attributes, such as speed limit and number of lanes. The AES trip was modeled to involve four steps: 1) a passenger appears in the network and walks to the nearest stop; 2) the passenger requests a pick-up, the closest available AES dispatches to pick up the passenger and drop the passenger off at the designated AES stop nearest the traveler's destination; 3) the passenger walks to the final destination; and 4) the AES waits at that destination stop until another pickup request is received and the AES is assigned to another traveler. The waiting time of the AES is basically relevant to the traffic demand of passengers (i.e., high demand may imply a short waiting time and low demand leads to a long waiting time). The simulation is set so that, once the passenger submits a request for a ride, the vehicle responses immediately and starts moving toward the passenger stop. After the vehicle completes a ride request, it will stop at the delivery stop of the last passenger and wait until it receives another request. This on-demand logic is very similar to today's elevator's technology logic. The time between the start of another trip and the stop of the previous trip could be defined as the waiting time of AES. The experiment in the paper gave a travel demand level of 300, which has a waiting time for an AES ranging from 1 to 12 seconds. There might be a small delay between submitting a ride request and the response from the vehicle due to communication delays and data processing. However, it is expected that this time delay to be very small compared to the waiting time for both the vehicle and passenger. For charging infrastructure design purposes, the worst case is considered in this work by neglecting the data processing and communication time delays, which lead to less wireless energy transfer at stops and increase the challenges for the charging infrastructure to meet the vehicle's energy requirements. Furthermore, in this study, the capacity of each AES is one passenger at a time.

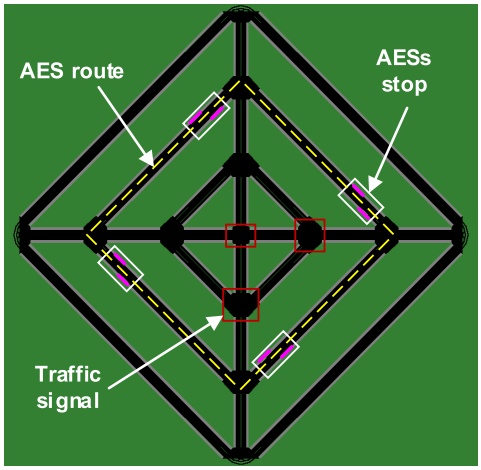

FIGURE 1. A hypothetical AMD network in SUMO.

The simulation was carried out for demand of 300 trips distributed across the 13 origin-destination (OD) pairs. Within this district simulation, all ODs are within feasible walkable distances, and the walk mode is for door-to-door trip completion. The choice set of travel modes encompasses 1) passenger car, 2) AES, and 3) walking. Traffic demand is distributed according to a bimodal distribution reflecting morning and afternoon peak hours during a typical day. After running the simulation, the driving data (e.g., speed and geographical location) of the four AESs are extracted to be utilized for investigating the required charging infrastructure. The speed profiles for the four AESs are shown in Fig. 2.

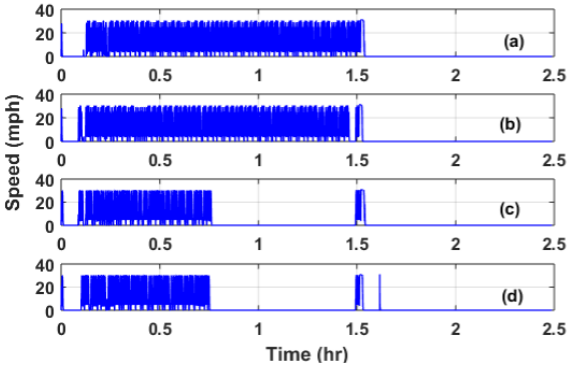

FIGURE 2. Speed profiles of the four AESs operating in the middle loop of the AMD network: (a) AES0, (b) AES1, (c) AES2, (d) AES3.

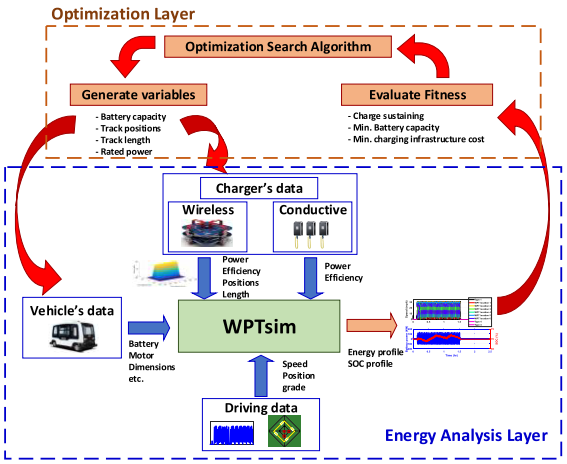

FIGURE 3. WPTSim-based WCI design platform.

III. SYSTEM DESIGN OF WIRELESS CHARGING INFRASTRUCTURE

A WPT simulation and system design optimization platform, called WPTSim, investigating WCI for fixed-route traffic scenarios has been developed. The platform has two layers: an energy analysis layer, and optimization layer, as indicated in Fig. 3. The energy analysis layer incorporates a vehicle energy consumption model, traffic data, and a charger model. This layer takes input data associated with a vehicle (battery capacity, mass, motor, etc.), traffic (speed, route, grade, etc.) and charger (rate, location, type, efficiency, etc.). It predicts the total vehicle energy and state-of-charge (SOC) profiles, considering vehicle dynamics (motoring and regenerative braking) and the charging events. The optimization layer provides an automatic search capability that changes the input parameters based on predefined objectives and constraints, and evaluates the output until the best combination of parameters is determined.

A. VEHICLE ENERGY CONSUMPTION MODEL

An energy consumption model for the SAEV is developed based on the Future Automotive Systems Technology Simulator (FASTSim) for vehicle powertrain modeling [31]. The model receives traffic data (vehicle speed and route) and vehicle parameters, such as aerodynamic drag, frontal area, mass, rolling resistance, etc., and generates the battery energy due to motoring and regenerative braking. At each time step, it estimates the road load power (P_E), including drag power (P_{drag}), acceleration power (P_{acc}), and ascent power (P_{asc}), as given in (1)-(4).

$$P_{drag}(\tau) = \frac{0.5\, D_{air} * C_{drag} * A_f * \left(\frac{s(\tau-1)+s(\tau)}{2}\right)^3}{1000} \quad (1)$$

$$P_{acc}(\tau) = \frac{\left(\frac{M_{tot}}{2\tau}\right) * \left(s(\tau)^2 - s\,(\tau-1)^2\right)}{1000} \quad (2)$$

$$P_{asc}(\tau) = \frac{G.sin\,(atan(g(\tau))) * M_{tot} * \left(\frac{s(\tau-1)+s(\tau)}{2}\right)}{1000} \quad (3)$$

$$P_E(\tau) = P_{drag}(\tau) + P_{acc}(\tau) + P_{asc}(\tau) \quad (4)$$

where D_{air} is the air density (1.225 kg/m^3), while C_{drag} is the vehicle drag coefficient, and A_f is the vehicle frontal area (m^2); τ represents the time step (sec); s $(\tau - 1)$ is the previous vehicle speed achieved [Mps (meters per second)], while $s(\tau)$ is the current vehicle speed (Mps). M_{tot} indicates the total vehicle mass including the battery mass (kg); G is gravity (9.8 m/sec^2), and g denotes the percentage of road grade.

In this work, the parameters of the EasyMile EZ10 autonomous electric shuttle are considered for vehicle modeling. It has a seating capacity of 12 passengers with 2,750 kg curb-weight and 19-kWh battery capacity, as presented in Table I [32].

TABLE 1. EasyMile EZ10 autonomous electric shuttle parameters.

Parameter	Value
Actual battery capacity	19 kWh
Base mass (M)	2,670 kg
M_b/kWh	10
Drag coefficient (C_{drag})	0.6
Auxiliary load, vehicle running	1.2 kW
Auxiliary load, vehicle parked	0.1 kW
Frontal area (A_f)	5.5 m^2

B. WIRELESS CHARGER MODEL

A wireless charger basically consists of two isolated sides: transmitter (track) and receiver (pick-up). Typically, the transmitter is embedded in the road, and the receiver is installed underneath the vehicle and attached to its chassis. The power transfers from the transmitter to receiver through a relatively large air-gap by magnetic field coupling. A model for the wireless charger was created and incorporated with the vehicle energy consumption model. The model determines the received electric power at the vehicle pad (receiver) based on the vehicle's position in the travel and lane directions. This power profile is a function of the coils' dimensions and shapes. According to the literature, there are two designs for the track with respect to the pick-up coil [33]: 1) long

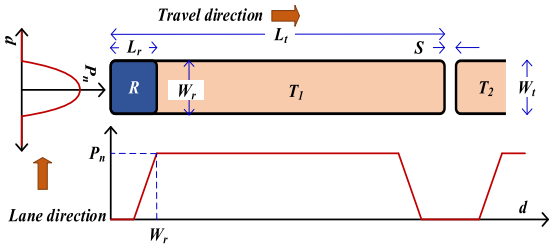

FIGURE 4. Coupled wireless power profile in travel and lane directions for long-track design with the system parameters.

TABLE 2. Parameters of one segment of DWPT system.

Parameter	Value
Maximum power (P_n)	100 kW
Segment Track length (L_t)	500 cm
Track width (W_t)	115 cm
Receiver length (L_r)	50 cm
Receiver width (W_r)	115 cm

track approach, and 2) multiple-pads approach. In the long track structure, the track length is longer than the pick-up coil length, which provides a higher and more constant power transfer profile. However, it shows less efficient operation due to the energization of a long cable with only a small portion coupled with the vehicle coil. On the other hand, the multiple-pad short track design can provide higher peak efficiency. However, it indicates a pulsating power profile with less energy transfer and higher installation costs. Due to the advantages of the long track design, it is considered in this study. For the long track design, the coupled power profile in the travel direction is trapezoidal with idle ends, as indicated in Fig. 4 [26], [34]. Also, the misalignment in the lane direction is considered by applying the parabola profile. The coupling power profile in both travel and lane directions for one segment of a 100-kW DWPT system with the characteristics presented in Table II is shown in Fig. 5. This figure is implemented in the design tool as a look-up table, which predicts the received power at the vehicle pad based on the misalignments in both travel and lane directions. These misalignments are measured by the distances between the center of the vehicle pad, which is assumed to match with the vehicle position provided by traffic simulation, and the center of the transmitter pad, which is known after defining the track positions, as will be explained in the next section.

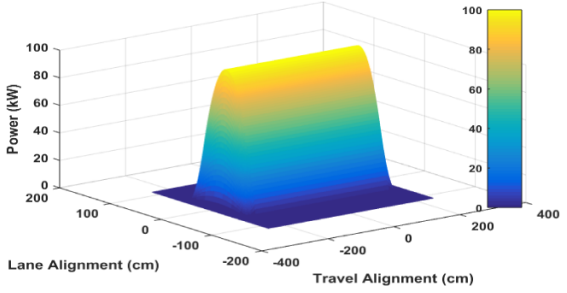

FIGURE 5. Coupled wireless power profile in travel and lane directions for 100-kW DWPT system with the parameters in Table I.

IV. DESIGN METHODOLOGY AND CASE STUDY

In this work, a design methodology based on the WPTSim tool in Fig. 3 for wireless charging infrastructure to serve fixed-route SAEVs in an AMD is presented. The wireless charging infrastructure design approach is explained in the following steps:

1) Integrate the input control parameters, including the driving data from SUMO (speed profile and route), wireless charger specifications, and vehicle parameters.
2) Assign potential positions for wireless chargers located on the vehicle's routes.
3) Choose and adjust the desired design variables, such as battery capacity, charging power level, track length, track positions, etc.
4) Run the WPTSim tool and check the energy and SOC profiles to evaluate the design.

In addition, the tool provides the capability to consider a conductive charging option at the parking spot or not. This charger is defined by its rated power and efficiency.

A. DESIGN CASE STUDY

The hypothetical AMD scenario with an AES (AES0) speed profile is considered with EasyMile EZ10 AS parameters. Based on the routes of the four AESs operating in the middle loop of the hypothetical network, 12 potential positions for in-route wireless chargers are defined, as depicted in Fig. 6. Four of these positions are quasi-dynamic (highlighted in green), which are aligned with the four stop stations. The other eight positions are dynamic and highlighted in blue. These 12 positions cover almost all of the entire middle loop of the network. The driving performance is analyzed using WPTSim where the 12 wireless charging positions are active with three track segments (15 meters, as indicated in Fig. 4 and Table II) at each position. The number of segments and the track length are decided to cover the entire bounded region for a wireless charger. For example, the quasi-dynamic positions (P1–P4) were set to supply 20 kW maximum power, while the dynamic positions (P5–P12) were established to transfer 40 kW. Moreover, in this case, a

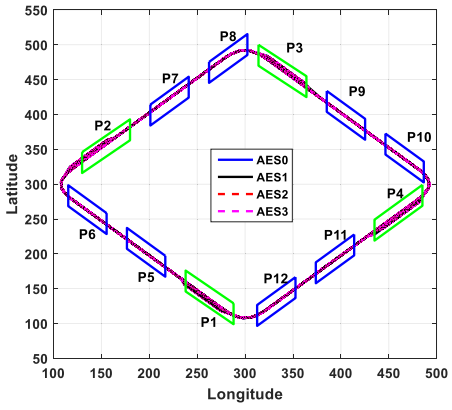

FIGURE 6. Placement of wireless transmitters along the middle loop, considering the routes of AES0, AES1, AES2 and AES3.

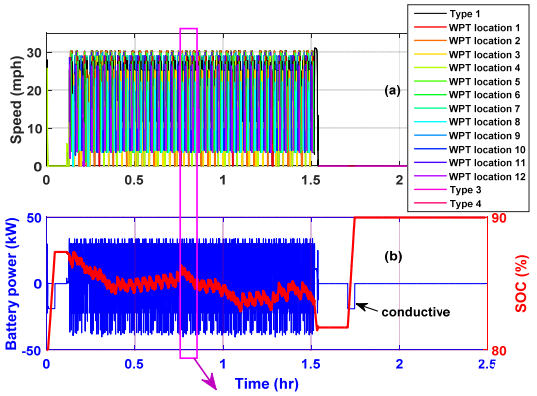

FIGURE 7. Driving performance with 12 wireless charging positions. (a) Speed profile showing different segments. (b) Battery power and SOC.

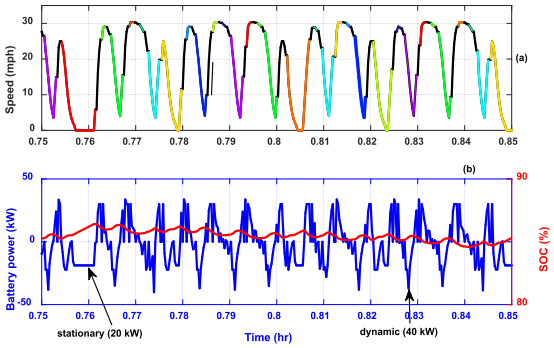

FIGURE 8. Zoomed driving performance with 12 wireless charging positions. (a) Speed profile showing different segments. (b) Battery power and SOC.

20-kW conductive charging capability was considered during the after-operation hours.

The driving performance in this scenario is indicated in Figs. 7 and 8. As it can be noticed in Fig. 7(a) and 8(a), the WPTSim tool divided the speed profile into segments and assigned a different color and type for each segment. Type 1 (black) was assigned to the segments where the vehicle runs without wireless charging. Type 2, with 12 different colors, was assigned to the segments in which the vehicle runs over a wireless charger. Type 3 (pink) was assigned to the segment where the vehicle is parked before activating the conductive charger, and type 4 was allocated during the conductive charging operation. As it can be noticed in Fig. 8(b), about 20-kW WPT took place during zero speed (quasi-dynamic positions), and 40-kW WPT took place during driving (dynamic positions). Moreover, a 20-kW conductive charge was activated during parking after a pre-set delay time to fully charge the vehicle [Fig. 7(b)]. The SOC profile is presented in Fig. 7(b), which varies based on the vehicle dynamics and charging events.

Manual parametric analysis can be performed by adjusting the input parameters for the vehicle and charger and evaluating the driving performance. However, doing this manual adjustment would be very difficult and time consuming due to a large number of variables. Furthermore, even with in-depth and intensive analysis, finding the best solution is not guaranteed due to the nonlinear relationships among the key variables. Therefore, an automatic optimization framework is necessary to find the best combination solution of the key design parameters that realizes predefined objectives and constraints.

V. DESIGN MULTI-OBJECTIVE OPTIMIZATION

Finding the best combination solution for the key design variables requires formulating and solving a multi-objective automatic optimization problem. Therefore, an optimization layer (as depicted in Fig. 3) was added on top of the energy analysis layer to provide an automatic search capability to find the optimal design parameters. An optimization search algorithm is integrated with the vehicle energy and charger models to iteratively generate the design variables, update the input data, get energy profiles and then evaluate the objectives and constraints. Based on the fitness (cost) function value, the algorithm produces a new combination of the design variables and continues repeating this process until the optimum solution is realized.

A. PROBLEM FORMULATION

The primary purpose of the optimization problem is to find the best combination of the design variables (e.g., battery capacity, WPT system parameters, etc.), such that the predefined objectives (e.g., charge sustaining operation, minimum battery capacity, etc.) are realized under certain constraints for a better battery performance. The multi-objective optimization problem for the WPT system with the hypothetical AMD scenario is formulated as follows:

1) OPTIMIZATION VARIABLES

Four design variables are investigated that represent the trade-off between minimizing the infrastructure cost and achieving charge sustaining operation. These design variables with their upper and lower limits are listed below.

1) Number and placement of each wireless charger (N_{WPT}): $x_1 \epsilon [1:4095]$.
2) Nominal power of wireless transmitter (P_T): $x_2 \epsilon \{10, 20, 30, \ldots, 100\}$ kW.
3) EV's battery capacity (Q_b): $x_3 \epsilon [2:60]$ kWh.
4) Number of track segments per position (N_S): $x_4 \epsilon [1:3]$ with 5 meters per segment (L_S) (i.e. [5 m: 15 m]).

The first variable (N_{WPT}) indicates the number of wireless charger positions and where these positions are located. It represented in the algorithm by a binary vector with 12 bits $\{b_1, b_2, \ldots, b_{12}\}$ (number of total candidate positions in order). In each iteration, the algorithm generates a real number between 1 and 4,095 (2^{12}-1), which is converted to a binary vector. The positions corresponding to ones are considered as active (transmitting power) and the positions corresponding to zeros are treated as inactive (do not exist). For example, if the algorithm generates 3,860, this

corresponds to 111100010100 and means that positions {1, 2, 3, 4, 8, 10} will be considered as active.

2) OPTIMIZATION OBJECTIVES

To solve the tradeoff between minimizing the DWPT infrastructure cost and achieving the two primary goals for this technology (realizing charge sustaining and reducing battery capacity), a multi-objective optimization with four objectives is identified. Due to the limited information about the actual cost components of the DWPT system, it is assumed that the total system cost is linearly proportional to the system design parameters (power level, battery capacity, and track length). In this case, three of the objectives that represent the DWPT cost are stated as linear functions of the design parameters.

a: PER-UNIT BATTERY CAPACITY

The first goal is to minimize the battery capacity required in the autonomous vehicle. This objective is stated mathematically as in (5).

$$f_1 = \left(\frac{Q_b}{Q_{b\_max}}\right) \quad p.u. \tag{5}$$

where Q_{b_max} is the upper boundary of the battery capacity (Q_b) in kWh.

b: PER-UNIT WIRELESS TRACK LENGTH

The infrastructure cost of the DWPT technology is proportional with the track length. Therefore, minimizing the length of the track embedded in the roadway is considered as a second objective, as given in (6).

$$f_2 = \frac{L_T}{L_{T\_max}} \quad p.u. \tag{6}$$

where L_T is the total embedded length of wireless track in meters, and L_{T_max} is the maximum possible length of the wireless track in meters. These lengths are formulated as a function of the number of wireless positions (N_{WPT}), number of track segments per position (N_S) and segment length (L_S), as given in (7).

$$\begin{aligned} L_T &= N_{WPT} \times N_S \times L_S \\ L_{T\_max} &= N_{WPT\_max} \times N_{S\_max} \times L_S \end{aligned} \tag{7}$$

where N_{WPT_max} is the number of all potential WPT positions (12 positions), and N_{S_max} is the maximum number of track segments that can fit at each position (three segments).

c: PER-UNIT WIRELESS CHARGER POWER

The component costs of the DWPT system are relevant to the power level. A high power level requires more magnetic materials, more litz wires, thicker wires, larger and more expensive power converters, and passive components. Reducing the power level will decrease the overall system cost, but it may not satisfy the vehicle's energy need. Therefore, the third objective in the formula is to optimize the charging power level, as stated in (8).

$$f_3 = \frac{P_T}{P_{T\_max}} \quad p.u. \tag{8}$$

where P_{T_max} is the upper boundary of the wireless charging rate P_T in kW.

d: CHARGE SUSTAINING OPERATION

Charge sustaining operation can be determined by reaching zero net energy at the end of the driving cycle, such that the consumed energy by the vehicle is compensated by the gained energy from the regenerative braking and wireless charging infrastructure. Consequently, the fourth objective in this problem is to minimize the net energy, as stated in (9).

$$f_4 = \frac{\left|E_f - E_i\right|}{E_i} \tag{9}$$

where: E_f and E_i are the final and initial battery energy in kWh, respectively.

3) OPTIMIZATION CONSTRAINTS

The optimization search algorithm is operated under certain constraints that restrict the charging and discharging operation, as stated in (10). The first two constraints (C_1 and C_2) were set to improve the EV's battery performance by avoiding over-charging and deep-discharging. A third constraint (C_3) was formulated to limit the search space to the solutions that have the potential to achieve charge-sustaining operation. The last set of constraints define the upper and lower limits of the optimization variables.

$$\begin{aligned} C_1&: \quad SOC_{min} \geq A\% \\ C_2&: \quad SOC_{max} \leq B\% \\ C_3&: \quad \left|SOC_{final} - SOC_{initial}\right| \leq \varepsilon\% \\ C_4&: \quad x_i^{(L)} \leq x_i \leq x_i^{(U)}, \quad i = 1, 2, 3, 4 \end{aligned} \tag{10}$$

where, A is the minimum acceptable SOC, B is the maximum acceptable SOC, ε is the maximum allowed the absolute difference in SOC, and x refers to an optimization variable, which has $x_i^{(U)}$ as an upper boundary and $x_i^{(L)}$ as a lower boundary.

B. OPTIMIZATION PROBLEM SOLUTION

The four objectives are addressed using the weighted sum technique, as indicated in (11).

$$\text{Minimize F}(x) = \sum_{m=1}^{4} w_m \; f_m(x) \tag{11}$$

where, w_m is the weight vector.

Considering linear relationships between the system cost and design parameters, equal-unity weights are assigned for all the objectives. In this case, it is assumed that all the objectives have the same degree of importance.

The optimization problem is solved using a genetic algorithm (GA), which is a stochastic search approach

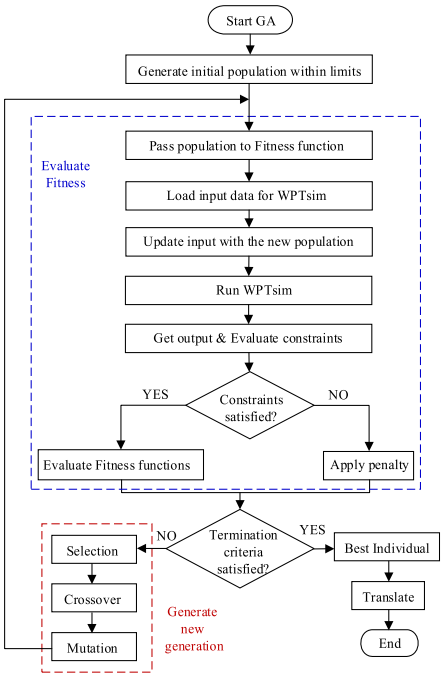

FIGURE 9. Flow-chart for the integration between GA and WPTSim.

TABLE 3. GA optimization settings.

Parameter		Value	Parameter	Value
Bounds	Variable	$[N_{WPT}, P_T, Q_b, N_S]$	A	40
	Lower	[1, 10, 1, 1]	B	80
	Upper	[4095, 100, 60, 3]	ε	5
Populations		40	$Q_{b\ max}$	60 kWh
Mutation		Uniform 80%	N_{WPT_max}	12 positions
Crossover		0.8	N_{S_max}	3 segments
Generation		50	L_S	5 meters
Number of running		3	P_{T_max}	100 kW
Penalty		1000		

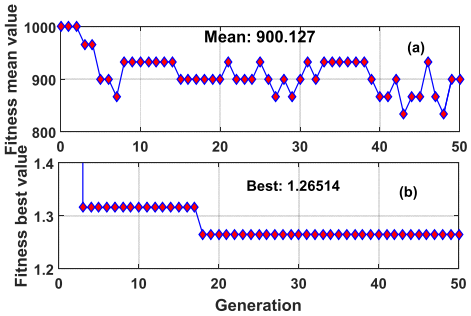

FIGURE 10. Progression of GA optimization. (a) Mean fitness value. (b) Best fitness value.

that emulates biological evolutionary theories to solve optimization problems. It enables parallel search from a population of points. Based on the literature, GA illustrated excellent performance in solving nonlinear and multi-objective optimization problems [35]. GA optimization is integrated with WPTSim tool to solve the multi-objective DWPT design optimization problem. The interaction between GA and WPTSim tool is explained by the flow-chart shown in Fig. 9.

VI. RESULTS AND DISCUSSION

The multi-objective optimization was formulated to find the optimum design parameters that serve the four AESs operating in the diamond AMD network scenario. The optimization settings and results are discussed in this section. Moreover, the optimum solution is analyzed and evaluated in comparison with other solutions, including stationary WPT and DCFC.

A. GA OPTIMIZATION SETTINGS AND RESULTS

In the optimization process, the speed profile of the first AES, AES0, from the AMD scenario with EasyMile EZ10 vehicle parameters was considered. The setting for the objective function, constraints' parameters, and GA are stated in Table III. The accepted SOC window through the entire driving cycle is set to 40% (40%–80%) to avoid deep discharging and overcharging, and the maximum acceptable change of SOC (ε) is set to 5% to realize charge sustaining. These settings were chosen and optimized by trial and error.

GA optimization was run with the settings in Table III for 2,000 iterations (40 populations × 50 generations) and repeated three times to ensure the best solution. The progression of the fitness function is indicated in Fig. 10. It illustrates the wide variation of the mean fitness value due to the random search capability of GA. However, the best fitness value shows a stable descend trend towards the minimum fitness (optimal solution), compared with the initial value.

The final optimal solution generated by GA is presented in Table IV. As can be observed, the algorithm chose the first four positions for the wireless chargers that match the designated AES stops. This makes a lot of sense since the vehicles can receive more electric energy at these positions by spending longer times during the low-speed movement and transient stops. Also, the algorithm decided to go with the maximum power level (100 kW) and minimum track length (1 segment/position), which leads to minimum charging infrastructure cost. Finally, the battery capacity was minimized to 9 kWh instead of 19 kWh, as initially installed by EasyMile.

TABLE 4. Optimal design solution.

Parameter	Optimal value
WPT positions (N_{WPT})	3840 = 111100000000 = [1, 2, 3, 4]
Wireless charging rate (P_T)	100 kW
Battery capacity (Q_b)	9 kWh
Segments per position (N_S)	1 (5-meter track length)
Best total fitness	1.26514

B. ASSESSMENT OF THE OPTIMAL DESIGN SOLUTION

The optimal design variables presented in Table IV were fed into the WPTSim tool for evaluation. The performance of the EasyMile EZ10 vehicle with the AES0 driving profile is described in Figs. 11 and 12. Note that, only four positions

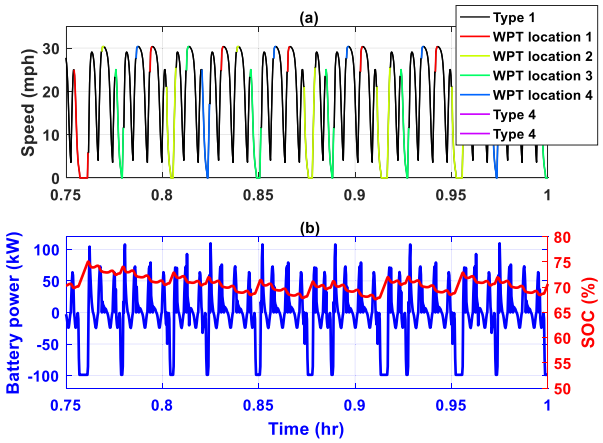

FIGURE 11. Optimal driving performance with four wireless charging positions and AES0 speed profile. (a) Speed profile showing different segments. (b) Battery power and SOC.

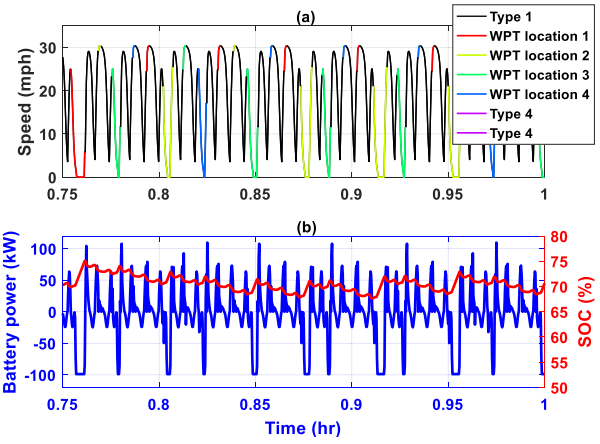

FIGURE 12. Zoomed optimal driving performance with four wireless charging positions and AES0 speed profile. (a) Speed profile showing different segments. (b) Battery power and SOC.

are assigned with Type 2 (existing over a wireless charger), and all charging events happened around zero speed with 100-kW rate. Moreover, Fig. 11(b) shows the SOC profile, which starts and ends almost at the same level, which proves the realization of charge sustaining operation.

The performance parameters are extracted from the optimum solution and presented in Table V. It can be observed that the SOC neither exceeded 80% nor dropped below 40% ($SOC_{max} = 79.14\%$ and $SOC_{min} = 59.37\%$). Also, the variation of SOC from the beginning to the end of the driving cycle is 0.04% (less than 5%).

TABLE 5. Performance parameters.

Parameter	Value
SOC_{max}	79.14%
SOC_{min}	59.37%
$SOC_{initial}$	70%
SOC_{final}	70.04%
$\lvert SOC_{final} - SOC_{initial} \rvert$	0.04%

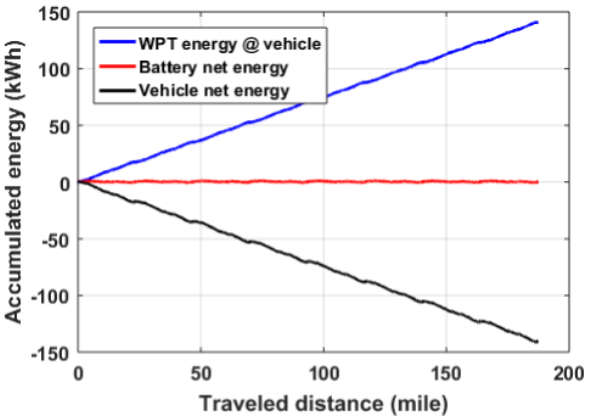

FIGURE 13. Energy profiles of the optimal design solution for about 200 miles range.

By repeating the active region of the speed profile of AES0, the driving range was extended from about 2.5 hr. (25 miles) presented in Fig. 7 to 12 hr. (about 200 miles). The energy profiles with the extended range are depicted in Fig. 13. The figure shows the energy profiles due to the vehicle dynamics (motoring and regenerative braking), in-route wireless chargers, and net battery energy. It can be noted that the vehicle energy consumption got compensated by WPT energy, such that the net battery energy is almost zero. This means that at the end of the driving cycle, the battery has the same energy level as when it started. Although only AES0 driving data have been considered in the optimization, the final solution is adequate for serving all AESs since they all have similar levels of energy consumption and speed. Moreover, they all are operating on-demand and using the four designated stops, which get electrified with wireless chargers.

C. BATTERY LIFE ASSESSMENT

Based on the design optimization results, increasing the charging power and decreasing the battery capacity and coil length lead to the most cost-effective design solution. However, this solution leads to a high battery charging rate (C-rate) of about 11C with an impulse charging profile, as indicated in Fig. 11. This results in a unique stress profile inside the battery cells that would impact the degradation mechanisms of the cells. Based on the literature, with proper battery design, thin-electrode graphite/nickel-manganese-cobalt (NMC532) lithium-ion batteries can tolerate up to 6C continuous charging for 800 cycles with just 10% capacity loss [36]. For a pulse charging profile within a narrow SOC window, these cells can presumably tolerate even more cycles. Furthermore, alternate anode chemistries, such as lithium titanate (LTO), are even better suited for frequent fast charging than graphite anodes. There are open questions regarding optimal battery design for cost, performance, and lifetime. These thin-electrode batteries may come with penalties of increased cost (as much as 100%) and reduced energy density (20%), however [37], lifetime is highly variable for different Li-ion cells. As a preliminary analysis, Fig. 14 shows lifetime

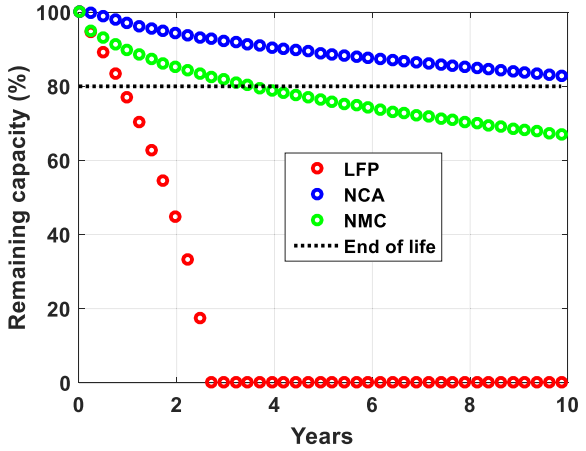

FIGURE 14. Estimates of battery lifetime under WPT use vary from 1 to 10 years across battery chemistries and designs.

predictions for four possible battery technologies under a WPT charging profile, shown in Fig. 11. This indicates that while batteries of specific chemistries, such as the Lithium Nickel Cobalt Aluminum Oxide (NCA), degrade less with the usage scenario considered here, other chemistries such as Lithium Nickel Cobalt Manganese Oxide (NMC) and Lithium Iron Phosphate (LFP) degrade much faster. The lifetime models were trained in various storage and low-rate cycling data. Actual outcomes for WPT cycling are uncertain. To reduce this uncertainty and better understand plausible WPT lifetime outcomes across battery chemistries and designs, further research is warranted to better understand battery lifetime under WPT applications, determine cost/life optimal battery designs for WPT, and include the battery life in the design optimization.

D. ASSESSMENT OF DIFFERENT CHARGING TECHNOLOGIES

By analyzing the range for the current AES EZ10 with a 19-kWh on-board battery and $SOC_i = 80\%$, the results show that a full charge cycle allows the vehicle to run continuously for less than 2 hrs., as indicated in Fig. 15. Therefore, this kind of vehicle requires either replacing the current battery with a larger one or deploying in-route wireless charging capability. In this section, a comparative analysis among three different scenarios is presented: 1) a large on-board battery with stationary wireless charger to be used at night, 2) a large on-board battery with DCFC to be used at night, and 3) a small on-board battery with the proposed in-route wireless charging. For the stationary charging options (1 and 2), the battery capacity is chosen to provide a 200-mile (12-hr.) range with a full charge cycle, and the charger power level is determined to fully charge the battery within 15 minutes, as a target by the U.S. Department of Energy (DOE) [37]. Under these conditions, the required battery capacity is about 300 kWh, and the charger nominal power is about 950 kW. The SOC profiles for the AES, considering the in-route and stationary charging options, are indicated in Fig. 15 in red and blue, respectively.

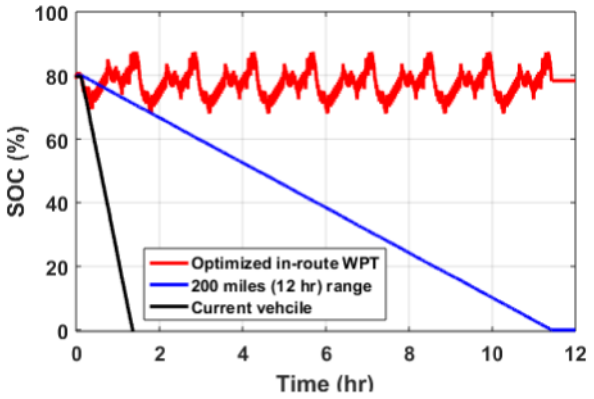

FIGURE 15. SOC profiles considering different charger and vehicle parameters (the current vehicle status, a vehicle with the optimized in-route WPT system and a vehicle with a 200-mile battery and 15-minute stationary charger).

TABLE 6. Performance matrix for different scenarios.

Performance parameter	*In-route WPT* (ΔSOC=20%)	*Stationary WPT* (ΔSOC=80%)	*Stationary DCFC* (ΔSOC=80%)
Vehicle component cost	Low (very small battery + 100kW VA)	High (very large battery + 950kW VA)	Medium (very large battery)
Road component cost	High (4x100kW WPT systems)	Medium (2x950 kW WPT systems)	Medium (2x950 kW DCFC)
Total cost	Medium	High	Medium
Land requirement	Low	High	High
Downtime	Zero	15 minutes	15 minutes
Range	Infinite	200 miles (12 hrs)	200 miles (12 hrs)
Energy consumption	Low (0.66 kWh/mile)	High (1.28 kWh/mile)	High (1.28 kWh/mile)
Automatic	Yes	Yes	NO
User discomfort	Low	Medium	High (mechanical connection)
Hazards	EMF	EMF	Mechanical connection, arcing, exposed conductor
Visual pollution	Low	Low	High

Table VI shows a comparative analysis for the three charging technologies, considering several performance indices, such as vehicle component cost (battery and vehicle assembly), road components cost (ground assembly and installation), vehicle range, downtime, energy consumption, etc. As it can be noticed, implementing in-route WPT system shows moderate total cost since the high road component cost is compensated with the low vehicle component cost. Additionally, it presents less energy consumption, zero downtime, infinite range and it is the most convenient for autonomous vehicles due to being automatic. The stationary WPT option shows that most expensive solution due to the requirement of large on-board battery and high-power ground assembly and vehicle assembly.

VII. CONCLUSION

The paper introduces an effective design methodology for the critical parameters of wireless charging infrastructure for SAEVs. The design approach is based on the WPTSim

tool, which integrates traffic data along with vehicle and charger energy models. The tool considered the impact of the misalignment in the travel and lane directions on the power transfer capability. A multi-objective optimization problem was formulated to solve the tradeoff between maximizing the benefits of wireless technology (achieving charge sustaining with minimum battery capacity) and minimizing the initial investment for constructing the wireless charging infrastructure. The optimization goal was to find the best combination of battery capacity and wireless charger characteristics (positions, length, and rate). The outcomes indicated that the proper design of parameters leads to a significant reduction in the battery capacity compared with the one installed by the manufacturer. They also show that few well-positioned wireless chargers with high rate and minimum length enable the vehicle to realize charge sustaining operation at the most cost-effective in comparison with the other charging technologies, including stationary WPT and DCFC. Even though in this study the proposed methodology is applied to a hypothetical AMD network, it is still applicable to different/larger networks. As long as the vehicle routes are known, the potential locations for wireless charging will be defined on these routes, and the algorithm will be able to optimize the design parameters based on the pre-defined objectives and constraints.

ACKNOWLEDGMENT

This work was authored by the National Renewable Energy Laboratory, operated by Alliance for Sustainable Energy, LLC, for the U.S. Department of Energy (DOE) under Contract No. DE-AC36- 8GO28308. The authors acknowledge John Smart of INL for leading the Alternative Fuel Infrastructure Pillar of the SMART Mobility Laboratory Consortium. The following DOE Office of Energy Efficiency and Renewable Energy (EERE) managers played important roles in establishing the project concept, advancing implementation, and providing ongoing guidance: David Anderson, and Erin Boyd. The views expressed in the article do not necessarily represent the views of the DOE or the U.S. Government. The U.S. Government retains and the publisher, by accepting the article for publication, acknowledges that the U.S. Government retains a nonexclusive, paid up, irrevocable, worldwide license to publish or reproduce the published form of this work, or allow others to do so, for U.S. Government purposes.

REFERENCES

[1] L. Fulton, J. Mason, and D. Meroux, "Three revolutions in urban transportation," ITDP, UC Davis, Academic Res., Davis, CA, USA, Tech. Rep., May 2017.
[2] Z. Lei, G. Venu, C. Yuche, H. Yi, H. M. A. Abdul, and Y. Stanley, "Quantifying the mobility and energy benefits of automated mobility districts using microscopic traffic simulation," in *Proc. Int. Conf. Transp. Develop.* 2018, p. 98.
[3] A. A. S. Mohamed, C. R. Lashway, and O. Mohammed, "Modeling and feasibility analysis of quasi-dynamic WPT system for EV applications," *IEEE Trans. Transport. Electrific.*, vol. 3, no. 2, pp. 343–353, Jun. 2017.
[4] Y. Zheng, Z. Y. Dong, Y. Xu, K. Meng, J. H. Zhao, and J. Qiu, "Electric vehicle battery charging/swap stations in distribution systems: Comparison study and optimal planning," *IEEE Trans. Power Syst.*, vol. 29, no. 1, pp. 221–229, Jan. 2014.
[5] M. Yilmaz and P. T. Krein, "Review of battery charger topologies, charging power levels, and infrastructure for plug-in electric and hybrid vehicles," *IEEE Trans. Power Electron.*, vol. 28, no. 5, pp. 2151–2169, May 2013.
[6] B. Walzel, C. Sturm, J. Fabian, and M. Hirz, "Automated robot-based charging system for electric vehicles," in *Proc. Internationales Stuttgarter Symp.*, 2016, pp. 937–949.
[7] J. Mardall and C. H. V. Dyke, "Charging station providing thermal conditioning of electric vehicle during charging session," U.S. Patent 0 306 974 A1, Oct. 29, 2015.
[8] S. Lukic and Z. Pantic, "Cutting the cord: Static and dynamic inductive wireless charging of electric vehicles," *IEEE Electrific. Mag.*, vol. 1, no. 1, pp. 57–64, Sep. 2013.
[9] A. A. S. Mohamed, A. Berzoy, F. G. N. De Almeida, and O. Mohammed, "Modeling and assessment analysis of various compensation topologies in bidirectional IWPT system for EV applications," *IEEE Trans. Ind. Appl.*, vol. 53, no. 5, pp. 4973–4984, Sep./Oct. 2017.
[10] A. A. S. Mohamed, F. G. N. De Almeida, and O. Mohammed, "Harmonics-based steady-state mathematical model of bidirectional inductive wireless power transfer system in V2G applications," in *Proc. IEEE Transp. Electrific. Conf. Expo (ITEC)*, Jun. 2016, pp. 1–6.
[11] Y. D. Ko and Y. J. Jang, "The optimal system design of the online electric vehicle utilizing wireless power transmission technology," *IEEE Trans. Intell. Transp. Syst.*, vol. 14, no. 3, pp. 1255–1265, Sep. 2013.
[12] B. Esteban, M. Sid-Ahmed, and N. C. Kar, "A comparative study of power supply architectures in wireless EV charging systems," *IEEE Trans. Power Electron.*, vol. 30, no. 11, pp. 6408–6422, Nov. 2015.
[13] A. A. S. Mohamed, S. An, and O. Mohammed, "Coil design optimization of power pad in IPT system for electric vehicle applications," *IEEE Trans. Magn.*, vol. 54, no. 4, pp. 1–5, Apr. 2018.
[14] G. A. Covic and J. T. Boys, "Inductive power transfer," *Proc. IEEE*, vol. 101, no. 6, pp. 1276–1289, Jun. 2013.
[15] C.-H. Ou, H. Liang, and W. Zhuang, "Investigating wireless charging and mobility of electric vehicles on electricity market," *IEEE Trans. Ind. Electron.*, vol. 62, no. 5, pp. 3123–3133, May 2015.
[16] K. Y. Kim, *Wireless Power Transfer: Principles and Engineering Explorations*. Rijeka, Croatia: InTech, 2012.
[17] C. Cai, J. Wang, Z. Fang, P. Zhang, M. Hu, J. Zhang, L. Li, and Z. Lin, "Design and optimization of load-independent magnetic resonant wireless charging system for electric vehicles," *IEEE Access*, vol. 6, pp. 17264–17274, 2018.
[18] L. Xiang, X. Li, J. Tian, and Y. Tian, "A crossed DD geometry and its double-coil excitation method for electric vehicle dynamic wireless charging systems," *IEEE Access*, vol. 6, pp. 45120–45128, 2018.
[19] F. Lu, H. Zhang, H. Hofmann, and C. Mi, "A dynamic charging system with reduced output power pulsation for electric vehicles," *IEEE Trans. Ind. Electron.*, vol. 63, no. 10, pp. 6580–6590, Oct. 2016.
[20] Z. Wang, S. Cui, S. Han, K. Song, C. Zhu, M. I. Matveevich, and O. S. Yurievich, "A novel magnetic coupling mechanism for dynamic wireless charging system for electric vehicles," *IEEE Trans. Veh. Technol.*, vol. 67, no. 1, pp. 124–133, Jan. 2018.
[21] Z. Chen, W. Jing, X. Huang, L. Tan, C. Chen, and W. Wang, "A promoted design for primary coil in roadway-powered system," *IEEE Trans. Magn.*, vol. 51, no. 11, Nov. 2015, Art. no. 8402004.
[22] W. Zhang, S.-C. Wong, C. K. Tse, and Q. Chen, "An optimized track length in roadway inductive power transfer systems," *IEEE J. Emerg. Sel. Topics Power Electron.*, vol. 2, no. 3, pp. 598–608, Sep. 2014.
[23] R. Tavakoli and Z. Pantic, "Analysis, design, and demonstration of a 25-kW dynamic wireless charging system for roadway electric vehicles," *IEEE Trans. Emerg. Sel. Topics Power Electron.*, vol. 6, no. 3, pp. 1378–1393, Sep. 2018.
[24] Y. J. Jang, S. Jeong, and Y. D. Ko, "System optimization of the on-line electric vehicle operating in a closed environment," *Comput. Ind. Eng.*, vol. 80, pp. 222–235, Feb. 2015.
[25] B. J. Limb, "Optimization of roadway electrification integrating wireless power transfer: TechnoEconomic assessment and lifecycle analysis," M.S. thesis, Dept. Mech. Eng., Utah State Univ., Logan, UT, USA, May 2017.
[26] A. Foote, O. C. Onar, S. Debnath, M. Chinthavali, B. Ozpineci, and D. E. Smith, "Optimal sizing of a dynamic wireless power transfer system for highway applications," in *Proc. IEEE Transp. Electrific. Conf. Expo (ITEC)*, Long Beach, CA, USA, Jun. 2018, pp. 1–6.
[27] K. Doubleday, A. Meintz, and T. Markel, "An opportunistic wireless charging system design for an on-demand shuttle service," in *Proc. IEEE Transp. Electrific. Conf. Expo (ITEC)*, Dearborn, MI, USA, Jun. 2016, pp. 1–6.

[28] A. Meintz, R. Prohaska, A. Konan, A. Ragatz, T. Markel, and K. Kelly, "Analysis of in-route wireless charging for the shuttle system at zion national park," in *Proc. IEEE PELS Workshop Emerg. Technol. Wireless Power Transf. (WoW)*, Knoxville, TN, USA, Oct. 2016, pp. 191–195.
[29] Y. Hou, S. E. Young, V. Garikapati, Y. Chen, and L. Zhu, "Initial assessment and modeling framework development for automated mobility districts: Preprint," Nat. Renew. Energy Lab., Golden, CO, USA, Tech. Rep. NREL/CP-5400-68290, Feb. 2018.
[30] D. Krajzewicz, J. Erdmann, M. Behrisch, and L. Bieker, "Recent development and applications of SUMO-simulation of urban mobility," *Int. J. Adv. Syst.*, vol. 5, no. 3, p. 4, 2012.
[31] A. Brooker, J. Gonder, L. Wang, E. Wood, S. Lopp, and L. Ramroth, "FASTSim: A model to estimate vehicle efficiency, cost and performance," in *Proc. SAE World Congr. Exhib.*, 2015, pp. 0148–7191.
[32] Home. *EasyMile*. Accessed: Sep. 25, 2018. [Online]. Available: http://www.easymile.com/
[33] Z. Zhang, H. Pang, C. H. T. Lee, X. Xu, X. Wei, and J. Wang, "Comparative analysis and optimization of dynamic charging coils for roadway-powered electric vehicles," *IEEE Trans. Magn.*, vol. 53, no. 11, Nov. 2017, Art. no. 9402106.
[34] M. Bertoluzzo, G. Buja, and H. K. Dashora, "Design of DWC system track with unequal DD coil set," *IEEE Trans. Transport. Electrific.*, vol. 3, no. 2, pp. 380–391, Jun. 2017.
[35] R. L. Haupt and S. E. Haupt, *Practical Genetic Algorithms*, 2nd ed. Hoboken, NJ, USA: Wiley, 2004.
[36] A. Jansen, "CAMP facility electrode and cell development for fast charge applications," in *Proc. UD Dept. Energy, Vehicle Technol. Office Annu. Merit Rev.*, Jun. 2018, pp. 5–10.
[37] D. Howell, S. Boyd, B. Cunningham, S. Gillard, and L. Slezak, "Enabling fast charging: A technology gap assessment," U.S. Dept. Energy, Office Energy Efficiency Renew. Energy, Washington, DC, USA, Tech. Rep. 10202017, Oct. 2017.

AHMED A. S. MOHAMED received the B.Sc. and M.Sc. degrees from the Electrical Power and Machines Department, Zagazig University, Egypt, in 2008 and 2012, respectively, and the Ph.D. degree from Florida International University (FIU), Miami, FL, USA, in 2017, all in electrical engineering.

From 2008 to 2013, he served as a Faculty Member with the Department of Electrical Power and Machines, Zagazig University. He is currently a Research Scientist with the National Renewable Energy Laboratory (NREL), Transportation and Hydrogen Systems Center, Golden, CO, USA. His research interests include wireless power transfer systems, power electronics, electric vehicles charging, and PV power systems. He is a Senior Member of IEEE. He was a recipient of the Outstanding Doctoral Student Award from FIU, in 2017.

ANDREW MEINTZ received the Ph.D. degree in electrical engineering from the Missouri University of Science and Technology, in 2011. He is a Senior Research Engineer with the National Renewable Energy Laboratory (NREL), Electric Vehicle Grid Integration Group. Prior to joining NREL, in 2014, he was a Battery Systems Engineer with General Motors with work on lithium-ion batteries for electric vehicles. His experience focused on advanced electric vehicle systems including fuel cells, power electronics, and battery systems from projects in both academia and industry.

LEI ZHU received the B.S. degree in electrical engineering from Dalian Maritime University, in 2006, the M.S. degree in electrical engineering from the University of Science and Technology of China, in 2009, and the Ph.D. degree in transportation engineering from The University of Arizona, in 2014. He is currently a Researcher with the National Renewable Energy Laboratory (NREL). His research focuses on automated mobility district modeling and simulation, connected and automated vehicles, ITS, GPS/GIS, big data in transportation, and traffic network modeling.